HHS Public Access

Author manuscript

*Circ Res*. Author manuscript; available in PMC 2021 July 03.

Published in final edited form as:

*Circ Res*. 2020 July 03; 127(2): e14–e27. doi:10.1161/CIRCRESAHA.119.315947.

# Depletion of Vasohibin 1 Speeds Contraction and Relaxation in Failing Human Cardiomyocytes

**Christina Yingxian Chen**[1,9], **Alexander K. Salomon**[1,9], **Matthew A. Caporizzo**[1], **Sam Curry**[1], **Neil A. Kelly**[1], **Kenneth Bedi**[2], **Alexey I. Bogush**[1], **Elisabeth Krämer**[4,5], **Saskia Schlossarek**[4,5], **Philip Janiak**[6], **Marie-Jo Moutin**[7,8], **Lucie Carrier**[4,5], **Kenneth B. Margulies**[2,1,3], **Benjamin L. Prosser**[1,3]

[1]Department of Physiology, Pennsylvania Muscle Institute, University of Pennsylvania Perelman School of Medicine, Philadelphia, PA, USA.

[2]Department of Medicine, University of Pennsylvania Perelman School of Medicine, Philadelphia, PA, USA.

[3]Penn Cardiovascular Institute, University of Pennsylvania Perelman School of Medicine, Philadelphia, PA, USA,

[4]Institute of Experimental Pharmacology and Toxicology, University Medical Center Hamburg-Eppendorf, Hamburg, Germany.

[5]DZHK (German Center for Cardiovascular Research), partner site Hamburg/Kiel/Lübeck, Hamburg, Germany.

[6]Cardiovascular Research, Sanofi R&D, Chilly-Mazarin, France.

[7]Grenoble Institut des Neurosciences (GIN), Université Grenoble Alpes, F-38000 Grenoble, France.

[8]Inserm, U1216, F-38000 Grenoble, France.

[9]These authors contributed equally: Christina Yingxian Chen, Alexander K. Salomon.

## Abstract

**Rationale:** Impaired myocardial relaxation is an intractable feature of several heart failure (HF) etiologies. In human HF, detyrosinated microtubules stiffen cardiomyocytes and impair relaxation.

**Address correspondence to**: Benjamin L. Prosser, Clinical Research Building Rm 726, 415 Curie Blvd., Philadelphia, PA 19104, bpros@pennmedicine.upenn.edu.

DISCLOSURES

Significant financial interests: Sanofi-Aventis, U.S., LLC – sponsored research >$50,000.

Invention disclosure/patent, inventor: composition and methods for improving heart function and treating heart failure. US patent application No.15/959,181 USA 2018.

Supplemental Materials

Online Figures I - III

Online Tables I – III

Full unedited blots

Major Resources Table

References 11, 16

Yet the identity of detyrosinating enzymes have remained ambiguous, hindering mechanistic study and therapeutic development.

**Objective:** We aimed to determine if the recently identified complex of VASH1/2 and SVBP is an active detyrosinase in cardiomyocytes and if genetic inhibition of VASH-SVBP is sufficient to lower stiffness and improve contractility in HF.

**Methods and Results:** Transcriptional profiling revealed that *VASH1* transcript is >10-fold more abundant than *VASH2* in human hearts. Using short hairpin RNAs (shRNAs) against VASH1, VASH2, and SVBP, we showed that both VASH1- and VASH2-SVBP complexes function as tubulin carboxypeptidases in cardiomyocytes, with a predominant role for VASH1. We also generated a catalytically dead version of the tyrosinating enzyme TTL (TTL-E331Q) to separate the microtubule depolymerizing effects of TTL from its enzymatic activity. Assays of microtubule stability revealed that both TTL and TTL-E331Q depolymerize microtubules, while VASH1 and SVBP depletion reduce detyrosination independent of depolymerization. We next probed effects on human cardiomyocyte contractility. Contractile kinetics were slowed in HF, with dramatically slowed relaxation in cardiomyocytes from patients with HF with preserved ejection fraction (HFpEF). Knockdown of VASH1 conferred subtle kinetic improvements in non-failing cardiomyocytes, while markedly improving kinetics in failing cardiomyocytes. Further, TTL, but not TTL-E331Q, robustly sped relaxation. Simultaneous measurements of calcium transients and contractility demonstrated that VASH1 depletion speeds kinetics independent from alterations to calcium cycling. Finally, atomic force microscopy confirmed that VASH1 depletion reduces the stiffness of failing human cardiomyocytes.

**Conclusions:** VASH-SVBP complexes are active tubulin carboxypeptidases in cardiomyocytes. Inhibition of VASH1 or activation of TTL is sufficient to lower stiffness and speed relaxation in cardiomyocytes from HF patients, supporting further pursuit of detyrosination as a therapeutic target for diastolic dysfunction.

## Graphical Abstract

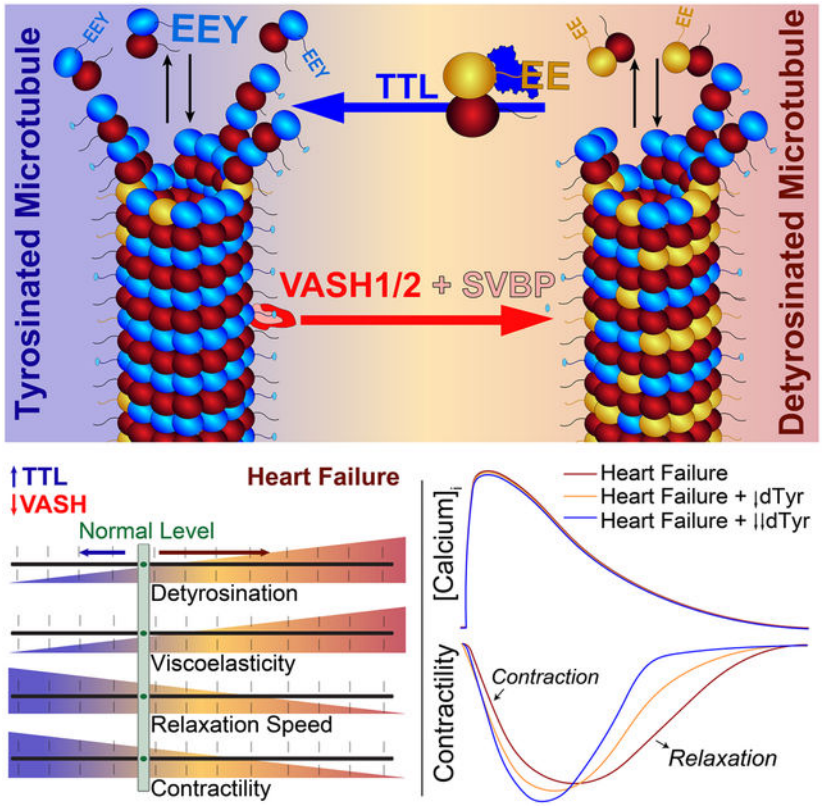


The microtubule cytoskeleton buckles and provides resistance to cardiomyocyte contraction, which is governed by the posttranslational tyrosination/detyrosination of α-tubulin. In heart failure, proliferation of detyrosinated microtubules increases cardiomyocyte stiffness and impairs contractility. Tyrosination is enzymatically catalyzed by tubulin tyrosine ligase (TTL), while detyrosination is catalyzed by a newly identified enzyme complex of VASH1/2 and SVBP, or by other, still unidentified detyrosinases. The tubulin detyrosinase has yet to be identified in the heart, which could provide a specific target for the treatment of heart failure. Here, we identified the VASH1/SVBP complex as a primary detyrosinase in cardiomyocytes. In cardiomyocytes from patients with heart failure, silencing of VASH1 lowered stiffness and partially restored contractile function. Silencing VASH1 specifically improved relaxation speed in failing human cardiomyocytes, without overtly altering the intracellular calcium transient. Speeding of relaxation was particularly pronounced in cardiomyocytes from patients with HFpEF, where impaired relaxation is a prominent and intractable clinical feature. In sum, our study identifies a prominent detyrosinase in cardiac muscle, and reveals that targeting this enzyme complex improves diastolic parameters in failing cardiomyocytes. This work pinpoints VASH1 as a new therapeutic target for the treatment of heart failure with diastolic dysfunction.

## Keywords

Microtubules; diastolic dysfunction; cardiomyocyte; relaxation

**Subject Terms:**

Basic Science Research; Cell Biology/Structural Biology; Contractile Function; Heart Failure; Myocardial Biology

## INTRODUCTION

Heart failure is often characterized by diastolic dysfunction, or inadequate ventricular filling due to the inability of the myocardium to fully relax. Diastolic dysfunction is a hallmark of hypertrophic cardiomyopathy (HCM)[1] and heart failure with preserved ejection fraction (HFpEF), diseases often characterized by prolonged and impaired left ventricular (LV) relaxation, slow LV filling, and increased diastolic LV stiffness.[2] Diastolic dysfunction can be initiated by factors extrinsic to the cardiomyocyte such as hypertension and fibrosis, or intrinsic impairments to cardiomyocyte calcium cycling and myofilament calcium sensitivity.

In addition to mechanisms that directly control sarcomere contraction and relaxation, myocyte motion can be modulated by the mechanical properties of the non-sarcomeric cytoskeleton. Cardiac microtubules provide viscoelastic resistance to myofilament shortening and re-lengthening through physical coupling of microtubules to the myofilaments.[3,4] This physical interaction is tuned by detyrosination, a post-translational modification of the C-terminal tail of α-tubulin (Figure 1A). In human heart failure (HF), the cardiac microtubule network proliferates and becomes more detyrosinated, increasing viscous drag on the myofilaments.[5] Multiple recent proteomic and biochemical assessments of patient myocardium suggest that detyrosinated microtubules are upregulated across the spectrum of end-stage HF,[5] as well as in patients with aortic stenosis[6] or inherited HCM.[7] Together, this data implicates microtubule detyrosination as a therapeutic target to lower stiffness and improve myocyte motion in HF.

Detyrosination can be genetically decreased by overexpression of tubulin tyrosine ligase (TTL), an enzyme highly specific for tubulin and responsible for ligating the terminal tyrosine residue back to detyrosinated tubulin.[8] Promisingly, overexpression of TTL in cardiomyocytes from patients with HF reduces cardiomyocyte stiffness, improves contractility,[3,5] and reduces cell stiffness during diastolic stretch.[4] However, the precise mechanism by which TTL modulates myocyte mechanics is unclear, as beyond its tyrosinating activity, TTL can also depolymerize microtubules by binding free tubulin dimers, preventing their incorporation into polymerized microtubules.[8,9] Because it is mechanistically unclear if TTL exerts its effect via changes in microtubule detyrosination, depolymerization, or both, methods to more specifically alter detyrosination are necessary to fully understand the mechanism of TTL action and to better define therapeutic targets for HF. Prior to the identification of tubulin carboxypeptidases responsible for detyrosination, tools to inhibit a detyrosinase have been limited to sesquiterpene lactones such as parthenolide, which must be used at high concentrations that elicit off target consequences.[5,10]

The recent identification of a detyrosinating enzyme complex of vasohibin-1 or −2 (VASH1/2) and their obligate partner small vasohibin binding protein (SVBP) potentially enables the development of more specific approaches to reduce detyrosination.[11,12] However, alternative tubulin carboxypeptidases beyond VASH exist in other cell types,[12] and it remains to be determined if either VASH1 or VASH2 are active detyrosinases in cardiomyocytes, and whether their selective inhibition is sufficient to improve contractility. In this study, we identify the VASH1-SVBP complex as a predominant tubulin carboxypeptidase in cardiomyocytes, and confirm that genetic depletion of VASH1 is sufficient to lower stiffness and improve contractility in cardiomyocytes from patients with HF. Further, we identify tyrosination-dependent and independent effects of TTL overexpression and find that tyrosination preferentially improves the relaxation kinetics of cardiomyocytes, and exerts its most profound effects on cardiomyocytes from patients with HF and diastolic dysfunction.

## METHODS

The authors declare that all supporting data are available within the article and its online supplementary files. For additional details in material and methods, please see the Major Resources Table in the Supplemental Materials.

### Human myocardial tissue.

Procurement of human myocardial tissue was performed under protocols and ethical regulations approved by Institutional Review Boards at the University of Pennsylvania and the Gift-of-Life Donor Program (Pennsylvania, USA) and as described.[5] Briefly, failing human hearts of non-ischemic origin were procured at the time of orthotropic heart transplantation at the Hospital of the University of Pennsylvania following informed consent from all participants. Non-failing (NF) hearts were obtained at the time of organ donation from cadaveric donors. In all cases, hearts were arrested in situ using ice-cold cardioplegia solution and transported on wet ice. Whole hearts and dissected left ventricle were weighed to determine levels of hypertrophy. Failing hearts are etiologically defined by clinical diagnosis of HF, which is subdivided into HFpEF (ejection fraction > 50%) and HFrEF (ejection fraction < 30%). Hearts were utilized for a particular experiment as they arrived until the required sample size was reached for each etiology of interest (e.g. triplicate quality isolations and experiments for NF, HFpEF and HFrEF).

For this study myocytes were isolated from 22 hearts (see method details below) for functional studies. For further details on classification, descriptive statistics, and experiments performed on each heart, see Online Table I.

### Human left ventricular myocyte isolation and cell culture.

Human left ventricular myocytes were isolated as described previously.[5] Culture medium consisted of F-10 (1X) Nutrient Mixture (Ham) [+] L-Glutamine (Life Technologies, 11550–043) supplemented with insulin-transferrin selenium-X (Gibco, 51500–056), 20 mmol/L HEPES, 1 μg $\mu l^{-1}$ primocin (Invivogen, ant-pm-1), 0.4 mmol/L extra $CaCl_2$, 5% FBS, and 25 μmol/L cytochalasin D (Cayman, 11330). Viable myocytes were concentrated

by gravity and the proper amount of medium was added in culture so that neighboring cells were not in direct contact. Viral constructs were permitted to express for 48 hours with a multiplicity of infection = 100–200.

### Animals.

Animal care and procedures were approved and performed in accordance with the standards set forth by the University of Pennsylvania Institutional Animal Care and Use Committee and the Guide for the Care and Use of Laboratory Animals published by the US National Institutes of Health.

### Rat cardiomyocyte isolation and culture.

Primary adult ventricular cardiac myocytes were isolated from 6 to 8 week old Sprague Dawley rats as previously described.[13] Briefly, the heart was removed from a rat anesthetized under isoflurane and retrograde-perfused on a Langendorff apparatus with a collagenase solution. The digested heart was then minced and triturated using a glass pipette. The resulting supernatant was separated and centrifuged at 300 revolution per minute (rpm) to isolate cardiomyocytes which were then resuspended in rat cardiomyocyte media at low density. Cardiomyocytes were cultured at 37°C and 5% $CO_2$ with 25 μmol/L of cytochalasin D. The viability of rat cardiomyocytes upon isolation is typically on the order of 50–75% rod-shaped, electrically excitable cells, and the survivability for 48hrs of culture is >80% (See Heffler et al.[14] for our quantification of cardiomyocyte morphology in culture). While the viability of human cardiomyocyte isolations is lower (with more variation between preparations), the 48hr survivability is similar to rat cardiomyocytes, and did not differ between experimental groups.

Rat cardiomyocyte media: medium 199 (Thermo Fisher 115090) supplemented with 1x Insulin-transferrin-selenium-X (Gibco 51500056), 1 μg $\mu l^{-1}$ primocin (Invivogen ant-pm-1), 20 mmol/L HEPES at pH 7.4 and 25 μmol/L cytochalasin D.

### Contractility and Calcium transient measurement.

Experiments were performed as previously described.[5] Briefly, prior to contractility measurement, cultured human myocytes were transferred to fresh warm medium without cytochalasin D. Contractility was measured in a custom-fabricated cell chamber (IonOptix) mounted on an LSM Zeiss 880 inverted confocal microscope using either a 40 or 63 X oil 1.4 numerical aperture objective and transmitted light camera (IonOptix MyoCam-S). Experiments were conducted at room temperature and field stimulation was provided at 0.5 Hz with a cell stimulator (MyoPacer, IonOptix). After 10–30 seconds of pacing to achieve steady state, five traces were recorded and analyzed. Sarcomere length was measured optically by Fourier transform analysis (IonWizard, IonOptix).

For simultaneous calcium and contractility measurement, myocytes were incubated with 2 μmol/L fluo-3-acetoxymethyl ester (Invitrogen) on rocker for 10 minutes at room temperature, then enriched by gravity for 5 minutes and replenished with fresh warm medium without cytochalasin D. Sarcomere length and fluo3 fluorescence were measured in a custom-fabricated cell chamber (IonOptix) mounted on a Zeiss inverted microscope using

a 40 X water 1.2 numerical aperture objective and CCD video camera (MyoCam-S3) coupling to a cell framing adaptor that connects to a photomultiplier tube (PMT400 Sub-System, IonOptix). Cell framing box for fluorescence detection was set at a fixed size. Fluorescence level of a blank area in the dish was recorded to account for background noise. Myocytes were electrically paced at 0.5 Hz at room temperature and both sarcomere length and fluorescence counts were recorded simultaneously for five steady-state transients.

### Generation of short hairpin RNAs.

Adenoviruses encoding shVASH and shSVBP constructs were generated and produced in a similar manner as previously described[3], but directed towards single target sites under the U6 promotor in three separate viruses. Target sites for VASH1: sh1: gctgcagtacaatcacacagg, sh2: gggacacagttctttgaaatt, sh3: gggaatttacctcaccaacag; for SVBP: sh1: gacaaagagcagagatctatg, sh2: gcagcagcagtttgatgagtt, sh3: gcagcagtttgatgagttctg; for VASH2: sh1: gtcaagaaggtcaagattggg, sh2: ggtcaagattgggctgtacgt, sh3: gtcaagattgggctgtacgt. eBFP2 was used as a marker of transduction. For data in the primary figures, *VASH1* sh1, *SVBP* sh3, and *VASH2* sh2 were utilized.

### RNA isolation, cDNA synthesis, and RT-qPCR.

RNA was isolated from cardiomyocytes using RNAzol RT (Molecular Research Center RN190) following the manufacturer's instructions. Briefly, cardiomyocytes were lysed in RNAzol RT reagent. One ml of the lysate was combined with 0.4 ml of water and shaken vigorously for 15 seconds and stored for 15 minutes at room temperature. Samples were then centrifuged at 12,000 g for 15 minutes. The supernatant was removed to a new tube and mixed with one volume of isopropanol, stored at room temperature for 10 minutes, then centrifuged at 12,000 g for 10 minutes. The RNA pellet was then washed with 75% ethanol two times and solubilized in RNase-free water. RNA concentration was determined using a Nanodrop (ThermoFisher) and 2μg RNA was reverse transcribed using cDNA synthesis kit (TaKaRa #6110A or SuperScript IV Thermo Fisher #18091150) following manufacturer's instructions. Twenty ng of cDNA template was then used to conduct RT-qPCR in three technical replicates. For *Vash1* and *Svbp* knockdown data sets, Powerup SYBR green master mix (#A25742, Thermo Fisher) was used with the following primers and thermocycle conditions: *Gapdh* (F-5'-CGTGCCGCCTGGAGAAAC-3' and R-5'-TGGGAGTTGCTGTTGAAGTCG-3'), *Vash1* (F-5'-TCGTCGGCTGGAAAGTAGGCAC-3' and R-5'-TCGTCGGCTGGAAAGTAGGCAC-3'), *Svbp* (F-5'-AACCAGCCTTCAGAGTGGAGAAGG-3' and R-5'-GCTCCGTCATGACTCTGTTGAGAGC-3'); Polymerase activation at 95 ˚C for 10 minutes and 40 cycles of denaturation at 95˚C for 15 seconds and annealing/extension at 60˚C for 1 minutes. For *Vash2* knockdown and relative transcript levels of *Vash1* and *Vash2* in rat myocytes, PrimeTime gene expression master mix (#1055772) with the following primers/probes and thermocycle conditions: *Vash2* (probe 5'-/56-FAM/TCAAGATCT/ZEN/TCATCCGCATGTCCCTG/3IABkFQ/−3', F-5'-GAAGCAACTTGTCCTCAATGTC-3' and R-5'-GGATTCTCACTTGGGTTGGAG-3') (assay name Rn.PT.58.45226291); *Vash1* (probe 5'−56-FAM/TGCCTACTT/ZEN/TCCAGCCGACAACG/3IABkFQ/−3', F-5'-GCCCAAGATTCCCATACCAA-3' and R-5'-ACTGTGTCCCTGTGTGATTG-3') (assay name Rn.PT.58.37363926); *Gapdh* (probe 5'-/56-FAM/CAGCACCAG/ZEN/

CATCACCCCATTTG/3IABkFQ/−3', F-5'-AACCCATCACCATCTTCCAG-3' and R-5'-CCAGTAGACTCCACGACATAC-3') (assay name Rn.PT.39a.11180736.g) (Integrated DNA Technologies); Polymerase activation at 95 ˚C for 3 minutes and 40 cycles of denaturation at 95˚C for 15 seconds and annealing/extension at 60˚C for 1 minutes. Cycle threshold (Ct) values were quantified on a QuantStudio 3 Real Time PCR system (ThermoFisher). Gene expression fold change was quantified using the delta-delta Ct method normalized to *Gapdh* and the scram group.

For RT-qPCR experiments in human samples, total RNA was extracted from septal myectomies of HCM patients (N=19), from explanted hearts of DCM patients (N=10) and from ischemic cardiomyopathy (ICM, N=10) patients as well as from NF human heart tissue not suitable for transplantation or from donors that did not die from cardiac disease but of another cause (NF, N=10–11) using the SV Total RNA Isolation Kit (Promega) according to the manufacturer's instructions and as described previously.[15] RNA concentration and purity was determined photometrically using the Nanodrop ND-1000. RNA was reverse-transcribed to cDNA using the Superscript III (Invitrogen) kit. Subsequently, RT-qPCR was performed using the Maxima SYBR Green/ROX qPCR Master Mix (Thermo Scientific) and the specific following primers and thermocycle conditions: *GAPDH* (F-5'-ATGTTCGTCATGGGTGTGAA −3' and R-5'- TGAGTCCTTCCACGATACCA −3'), *VASH1* (F-5'-AGAGGAAGGGGAAGAGGACC-3' and R-5'-GTAGGCACACTCGGTATGGG −3'), *VASH2* (F-5'- GTTCCACGTCAACAAGAGCG and R-5'- CGACAGCCTGTAGTTTGGGA −3'), *SVBP* (F-5'-CAGCAGAGTTGAGAAGGCCA −3' and R-5'- CCAGGAGGCTGCATCTGTTT −3'); Polymerase activation at 95 ˚C for 10 minutes and 40 cycles of denaturation at 95˚C for 15 seconds and annealing/extension at 60˚C for 1 minutes. Relative gene expression of *VASH1, VASH2* and *SVBP* was calculated using the delta Ct method (with a formula 2^ (-delta Ct)) normalized to *GAPDH*.

### Microtubule fractionation assay.

Isolated rat cardiomyocytes were pelleted by gravity, washed with warm microtubule stabilizing buffer containing 0.1 mol/L PIPES (pH 6.8), 2mmol/L EGTA, 0.1 mmol/L EDTA, 0.5 mmol/L $MgCl_2$, 20% glycerol, and centrifuged at 300 rpm for 2 minutes. The resulting pellet was resuspended in 150 µl microtubule-stabilizing buffer supplemented with 0.1% Triton X-100 and 1X protease and phosphatase Inhibitor cocktail (Cell Signaling #5872S) and incubated for 30 minutes at 37 °C. Next, cells were centrifuged at 300 rpm for 2 minutes and the supernatant was collected as the free tubulin fraction. The resulting pellet was resuspended in 150 µl RIPA buffer (Cayman #10010263) supplemented with extra 0.8% SDS, disrupted by pipetting every 15 minutes on ice for 1 hour, then boiled at 100 °C for 3 minutes. Finally, the fraction was centrifuged at 12,000 g for 2 minutes and the supernatant was collected as the polymerized fraction.

### Western blot.

For whole cell protein extraction, isolated rat cardiomyocytes were lysed in RIPA buffer (Cayman #10010263) supplemented with protease and phosphatase Inhibitor cocktail (Cell Signaling #5872S) on ice for 1 hour. The supernatant was collected and combined with 4X

loading dye (Li-COR #928–40004), supplemented with 10% 2-mercaptoethonol, and boiled for 8 minutes. The resulting lysate was resolved on SDS-PAGE gel and protein was blotted to nitrocellulose membrane (Li-COR #926–31902) with mini Trans-Blot Cell (Bio-Rad). Membranes were blocked for an hour in Odyssey Blocking Buffer (TBS) (LI-COR #927–50000) and probed with corresponding primary antibodies overnight at 4 °C. Membranes were rinsed with TBS containing 0.5% Tween 20 (TBST) three times and incubated with secondary antibodies TBS supplemented with extra 0.2% Tween 20 for 1 hour at room temperature. Membranes were washed again with TBST (0.5% Tween 20) and imaged on an Odyssey Imager. Image analysis was performed using Image Studio Lite software (LI-COR). All samples were run in duplicates and analyzed in reference to GAPDH.

### Antibodies and labels.

Detyrosinated tubulin; rabbit polyclonal (Abcam ab48389); western blot: 1: 1,000.

Alpha tubulin; mouse monoclonal, clone DM1A (Cell Signaling #3873); western blot: 1:1,000

TTL; rabbit polyclonal (Proteintech 13618–1-AP); western blot: 1:500.

GAPDH; mouse monoclonal (VWR GenScript A01622–40); western blot: 1:1,000.

IRDye 800CW Donkey anti-Mouse IgG (H + L) (LI-COR 925–32212); western blot: 1:10,000.

IRDye 680RD Donkey anti-Rabbit IgG (H + L) (LI-COR 925–68073); western blot: 1:10,000.

IRDye 680RD Donkey anti-Mouse IgG (H + L) (LI-COR 926–68072); western blot: 1:10,000.

IRDye 800CW Donkey anti-Rabbit IgG (H + L) (LI-COR 926–32213); western blot: 1:10,000.

VASH1; rabbit polyclonal (Abcam ab199732); western blot 1:5000–1:1000

A novel antibody for human and mouse VASH1 (named anti-VASH1 Gre) was produced in rabbits by using a peptide C-RIRGATDLPKIPIPSVPTFQPTTPV-NH2 (corresponding to exposed region of the protein, see Wang, Bosc and Choi et al.)[16] linked at the N-terminal to the keyhole limpet hemocyanin protein via the cysteine. Sera from rabbits were purified on the respective peptides. Validation of these antibodies was performed in HEK293T cells protein extracts (see Online Figure IIIA). HEK293T cultures and transfections, as well as SDS-PAGE and immunoblots, were performed as in Aillaud et al.[11]

### Co-immunoprecipitation (co-IP).

Isolated rat cardiomyocytes were lysed in IP buffer containing Tris 50mmol/L pH 8, NaCL 150mmol/L, NP40 1% and protease inhibitor cocktail (Cell Signaling #5872S) on ice for 30 minutes with pipetting every 10 minutes. Protein concentration was quantified using Braford

dye reagent (Bio-Rad #5000205). Equal amount of protein (1.5 mg) from each sample was incubated with 6.5μg of anti-SVBP (Gre) and 10μl of Dynabeads protein G (Invitrogen 10004D, rinsed four times with ice-cold PBS before used), mixed on a tube revolver (Thermo Fisher #11-676-341F5). Negative controls for co-IP were run with Rabbit IgG (6.5μg) or without antibody. After overnight incubation at 4˚C, beads were rinsed with IP buffer for four times and eluted at room temperature using 30μl 1X Laemli buffer (Bio-Rad) supplemented with 2-mercaptoethonol. Elution supernatant was then transferred to fresh tubes and heated at 70˚C for 5 min. Fifteen μl of the elution from co-IP and whole cells lysates were used in western blot, performed as described above except the followings. Blots were stained with anti-VASH1 (Gre) at 1:1,000 at 4˚C overnight and a secondary antibody against native rabbit IgG at 1:1,000 (TrueBlot anti-rabbit IgG HRP from Rockland #18-8816-31) at room temperature for 1 hour. Blots were developed using a chemiluminescent substrate (West Pico Plus, Thermo Fisher #34577) and autoradiography film (Hyblot CL #E3012).

### Nanoindentation.

Mechanical properties at the microscopic scale were measured using nanoindentation[4] (Piuma Chiaro, Optics11, The Netherlands). Freshly isolated human myocytes were attached to glass bottom dishes coated with MyoTak[13] in normal Tyrode's solution containing 140 mmol/L NaCl, 0.5mmol/L $MgCl_2$, 0.33 mmol/L $NaH_2PO_4$, 5 mmol/L HEPES, 5.5 mmol/L glucose, 1 mmol/L CaCl2, 5 mmol/L KCl, pH to 7.4 at room temperature. A spherical nano-indentation probe with a radius of 3.05 μm and a stiffness of 0.026 N $m^{-1}$ was used. Myocytes were indented to a depth of 1.5–3.5 μm with velocities of 0.1, 0.25, 0.5, 1.0, 2.0, 5.0, 10.0, 20.0, 50.0, 100.0, and 150.0 μm $s^{-1}$. The tip was held in this indentation depth for 1 s, and retracted over 2 s. The Young's moduli were calculated automatically by the software, by fitting the force versus indentation curve to the Hertz equation.

### Statistics.

Statistical analysis and graphing were performed using OrginPro software (OriginLabs). Values are presented as mean ± s.e.m. in line graphs and bar graphs (Figure 3D through F; Figure 4D), and when stated in the results. For box plots, box represents 25$^{th}$ to 75$^{th}$ percentiles, the whiskers 1 s.d. and mean line. Data was checked for normality via Kolmogorov Smirnov test within OriginPro. All experiments were replicated in multiple rat or human hearts (biologically independent samples/independent experiments) for each condition, indicated by the N number in each figure and figure legend. The exact n values used to calculate statistics and the statistical tests for significance are stated in individual graphs or figure legends. Two-sided t-tests were used to determined statistical significance between experimental conditions vs. control (Figure 1F; Figure 1G VASH2 KD). One-way analysis of variance (ANOVA) (Figure 1C and 1D; Figure 2B and 2C) or two-way ANOVA (Figure 3C) with post-hoc Bonferroni test. Given that multiple comparisons were both repetitive and restricted and could increase the chance of type 1 error (testing multiple parameters derived from one experiment e.g. contractility), the Bonferroni correction was applied after two-sided *t*-tests to adjust the significance threshold by dividing it with the number of tests, as described in each figure legend where appropriate, and unadjusted P values are reported in the figures (Figure 1B; Figure 3D through F; Figure 4B through 4D).

# RESULTS

## A note on human samples.

Twenty-two human hearts were used in this study for functional tests. All patient studies were conducted on explanted human hearts from patients with non-ischemic heart failure (hypertrophic or dilated cardiomyopathy, HCM or DCM, respectively). When sufficient samples were available, hearts were further sub-classified as either heart failure with reduced ejection fraction (HFrEF) for patients with left-ventricular ejection fraction (LVEF) below 30%, or HFpEF for those with LVEF above 50% at time of transplant. Non-failing (NF) donor hearts were used as controls. For relevant clinical characteristics please see Table 1, and for descriptions of experiments performed on each heart, please see Online Table I.

## TTL overexpression improves contractility in isolated cardiomyocytes from failing human hearts independent of changes to the calcium transient.

We previously showed that TTL overexpression reduces viscoelasticity and improves contractility in NF human cardiomyocytes.[5] Because the microtubule network increases in density and becomes highly detyrosinated during heart disease, we wanted to extend these studies to cardiomyocytes from failing hearts, and examine any effect of TTL overexpression on calcium handling. We transduced cardiomyocytes from patients with HF with adenovirus overexpressing TTL or a control virus (null), and assessed electrically stimulated $[Ca^{2+}]_i$ transients and sarcomere shortening. TTL overexpression robustly improved myocyte contraction and relaxation kinetics, with no detectable change to the kinetics or amplitude of the calcium transient (Figure 1B, Online Table II). These results are consistent with the hypothesis that reducing detyrosination improves the contractility of failing cardiomyocytes through mechanisms predominantly independent of a change in calcium cycling.

## Generation of constructs to isolate TTL tubulin sequestration from tyrosination.

Although TTL overexpression reduces the proportion of detyrosinated microtubules, the precise mechanism by which TTL improves contractility is not clear, as TTL can depolymerize the microtubule network via sequestration of free tubulin,[8] which is sufficient to improve contractility.[4] To isolate effects of TTL attributable to tubulin sequestration vs. tyrosination, we generated adenovirus encoding an established TTL catalytic-dead construct (TTL-E331Q) that binds tubulin with wildtype kinetics, but cannot enzymatically tyrosinate tubulin.[8] We validated this tool in healthy rat cardiomyocytes, where adenoviral overexpression of TTL-E331Q to the same level of TTL did not significantly reduce detyrosinated tubulin (Figure 1C).

## VASH1/SVBP is a predominant cardiac tubulin carboxypeptidase.

To interrogate detyrosination, independent of any potential microtubule depolymerization via TTL, we sought to directly manipulate a cardiac detyrosinase. We conducted experiments to verify if the recently identified VASH-SVBP complex is a primary detyrosinase in myocardium, to determine if any isoform of VASH is dominant, and whether VASH/SVBP expression changes in disease. Transcriptional profiling of healthy and

diseased human myocardium identified that *VASH1* has approximately 15-fold (±5) higher expression level than *VASH2* in NF tissue (Figure 1D). In isolated rat cardiomyocytes, we found *Vash1* to be expressed ~5 fold (±2.2) more than *Vash2* (Figure 1E). In diseased myocardium, *VASH1* gene expression was higher in dilated cardiomyopathy (DCM) and did not significantly change in ischemic cardiomyopathy or HCM, while *VASH2* gene expression was modestly decreased in HF (Figure 1D). When comparing the expression of *VASH1* to *VASH2* across all etiologies of HF, *VASH1* was expressed ~28–50 fold higher than *VASH2*. *SVBP* was consistently expressed at a high level and did not show differential expression with disease.

We also sought to evaluate protein abundance of VASH1/2 and SVBP, but were aware of the lack of well-validated antibodies for these targets (note the lack of any such antibodies used in recent publications identifying the role and structure of these enzymes). To address this, we generated new antibodies that were validated in parallel with commercial antibodies in vitro (please see Online Figure III for details). While the custom VASH1 antibody was indeed more sensitive and specific than commercially available options, we still were unable to detect a reliable band in cardiac cell or tissue lysate. Thus, further work is needed to detect these enzymes, which are likely of relatively low abundance in the cardiac proteome.

We next depleted VASH1, VASH2, and SVBP in healthy rat cardiomyocytes to determine if they function as tubulin carboxypeptidases. For each of these genes, we generated three adenoviruses encoding short hairpin RNAs (shRNAs) specific for three target sites conserved between rats and humans. Delivery of each of these shRNAs by adenovirus to isolated rat cardiomyocytes resulted in a reduction of detyrosinated tubulin, without changing total tubulin levels (Figure 1G; Online Figure I). We selected the shRNAs that resulted in the most robust and consistent decrease in detyrosinated tubulin levels and confirmed that they depleted *Vash1, Vash2* and *Svbp* transcripts via RT-qPCR (Figure 1F). With similar decreases in transcript levels (Figure 1F), VASH1 and SVBP KD induced an ~55% (± 5%) reduction in detyrosinated tubulin while VASH2 KD caused a ~25% (± 6.5%) reduction (Figure 1G). As SVBP depletion inhibits the functionality of both VASH1 and VASH2,[16–18] SVBP depletion would be predicted to lead to a greater reduction in detyrosinated tubulin than depletion of VASH1 or VASH2 alone. We did not observe this, which could be due to incomplete SVBP KD or SVBP-autonomous activity of VASH2, as indicated in a recent report.[19] Regardless, our results support a more prominent role of VASH1 in cardiomyocyte detyrosination, which is consistent with a recent patent[20] demonstrating that VASH1 KO robustly reduces detyrosinated tubulin in the heart, while VASH2 KO has a more modest effect. The fact that TTL overexpression reduces detyrosinated-tubulin by ~80% (± 5%) while VASH1/SVBP depletion lowers levels by ~55% is consistent with the abundant expression of TUBA4A in cardiomyocytes,[5,11] an α-tubulin isotype translated in its detyrosinated form, and thus insensitive to manipulation of a detyrosinase, but readily tyrosinated by TTL.

### Tubulin sequestration by TTL, and not VASH1/SVBP knockdown, decreases microtubule stability in healthy cardiomyocytes.

With these new tools generated, we next sought to determine the effect that TTL/TTL-E331Q overexpression or VASH1/SVBP knockdown has on the stability of the microtubule network. Using a fractionation assay that allows for separation of soluble, free tubulin from polymerized microtubules, we found that overexpression of TTL (~9 ± 2 fold) in healthy rat cardiomyocytes led to a robust (~80 ± 5%) reduction in detyrosinated tubulin that did not occur with TTL-E331Q (Figure 2A and 2B). Both TTL and TTL-E331Q overexpression increased the amount of free tubulin relative to polymerized microtubules (Figure 2A and 2C), indicating modest depolymerization of the microtubule network. In contrast, knockdown of either VASH1 or SVBP reduced the level of detyrosinated tubulin in polymerized microtubules (~40 ± 2%), yet the free:polymerized tubulin ratio remained unchanged (Figure 2A through 2C). These results suggest that tubulin binding via TTL is sufficient to depolymerize the microtubule network in isolated rat cardiomyocytes, and that modest reductions in detyrosination alone are not sufficient to depolymerize microtubules.

We noted that TTL overexpression or knockdown resulted in variable changes in the ratio of free:polymerized tubulin that seemed to mirror changes in detyrosination. Indeed, plotting the change in detyrosinated tubulin from each experiment against the change in free:polymerized tubulin revealed an inverse correlation with levels of detyrosination (Figure 2D), suggesting that decreasing detyrosination may decrease microtubule network stability in cardiomyocytes, but requires a threshold reduction in detyrosination. This would imply that any destabilizing effect of VASH1/SVBP depletion would be contingent on a sufficient initial proportion of detyrosinated microtubules in the network, such as occurs in HF.

### Effects of VASH1 knockdown and TTL-E331Q overexpression on myocyte contractility.

We next sought to determine how TTL/TTL-E331Q overexpression or VASH1 knockdown would affect the contractility of isolated cardiomyocytes from failing and NF hearts. In cardiomyocytes from NF donor hearts, VASH1 knockdown produced modest but consistent speeding of contraction and relaxation kinetics, and subtle effects on contractile amplitudes (Figure 3A through 3D; Online Table II). We also interrogated the effect of VASH1 depletion in cardiomyocytes from 6 patients with HF, 3 with HFrEF (systolic dysfunction), and 3 with HFpEF (diastolic dysfunction). As shown in the average traces of cardiomyocytes from these hearts transduced with control adenovirus (Figure 3B), failing heart cells exhibited lower contractile amplitudes and slower kinetics than NF controls. There was markedly slower relaxation in failing cardiomyocytes that was particularly evident in HFpEF cardiomyocytes (Figure 3C), consistent with the impaired relaxation implicated in this disease etiology. On average, relaxation velocity was 2.1-fold and 3.6-fold lower in HFrEF and HFpEF than in NF controls, respectively (scram groups: NF 1.51 ± 0.056, HFrEF 0.71 ± 0.083, and HFpEF 0.41 ± 0.041 μm/s). VASH1 depletion markedly improved contractile amplitudes and contraction and relaxation kinetics in failing cardiomyocytes, eliciting a 1.6 and 2-fold improvement in relaxation velocity in HFrEF and HFpEF cardiomyocytes, respectively (VASH1 KD groups: NF 1.79 ± 0.062, HFrEF 1.12 ± 0.099, and HFpEF 0.81 ± 0.065 μm/s; Figure 3A through 3D; Online Table II).

The effect of SVBP depletion was examined in cardiomyocytes from a separate subset of 3 failing hearts (2 HFrEF, 1HFpEF), where it elicited similar improvements in contraction and relaxation kinetics as VASH1 knockdown (Online Figure IIC and IID; Online Table II).

In NF cardiomyocytes, both TTL and TTL-E331Q overexpression improved most metrics of systolic function compared to cells transduced with control adenovirus, although improvements in relaxation time appeared to only be sensitive to TTL, and not to TTL-E331Q (Figure 3C and 3E). This became more apparent in cardiomyocytes from failing hearts (HFrEF), where both constructs improved systolic parameters, yet TTL had a significantly greater effect than its catalytically dead counterpart on relaxation time, and robustly improved relaxation velocity (Figure 3C and 3F).

Together, this data indicates that 1) relaxation kinetics are particularly slowed in failing cardiomyocytes; 2) selectively targeting microtubule detyrosination via either the tyrosinase or detyrosinase is sufficient to robustly improve relaxation kinetics; 3) the effect of reducing microtubule detyrosination is most remarkable in failing cardiomyocytes; and 4) the microtubule depolymerizing activity of TTL is sufficient to augment systolic, but not necessarily diastolic parameters.

### VASH-1 knockdown reduces myocyte stiffness and has negligible effects on $[Ca^{2+}]_i$ transients.

Typically, we conduct myocyte contractility assays in the absence of $Ca^{2+}$ indicator dye, as they can slow contractile kinetics due to $Ca^{2+}$ buffering and obscure kinetic phenotypes. For this reason, the $[Ca^{2+}]_i$ transient data in Figure 1B was collected on a separate subset of cardiomyocytes from those evaluated for contractility. Recognizing that inhibition of tubulin detyrosination with parthenolide has off target consequences on calcium handling in human cardiomyocytes,[5] we sought to more directly examine the relationship between calcium handling and contractility after VASH1 knockdown in myocytes. Thus, cardiomyocytes from a separate subset of 5 hearts were loaded with a low concentration of the $Ca^{2+}$ indicator dye fluo-3 and simultaneously assessed for $[Ca^{2+}]_i$ transients and contractility. As shown in the average trace of myocytes from a HFpEF heart (Figure 4A), VASH1 knockdown robustly improved fractional shortening, contraction and relaxation speed independent of any observable change in $Ca^{2+}$ handling in those same cells. This $Ca^{2+}$-independent improvement in contractility was observed in both NF and failing cardiomyocytes (Figure 4B and 4C).

In the absence of any demonstrable effect on $Ca^{2+}$ cycling, the observed improvement of systolic and diastolic kinetics with VASH1 knockdown are consistent with a reduction of viscoelastic resistance to sarcomere motion contributed by detyrosinated microtubules.[4] To test this hypothesis, we directly probed viscoelasticity via transverse nanoindentation of failing human cardiomyocytes with or without VASH1 knockdown. In response to very slow deformation, the Young's modulus of VASH1-depleted cells was unchanged, suggesting a minimal effect on transverse elasticity ($E_{min}$, Figure 4D). Yet at rates of deformation relevant to the cardiac cycle, VASH1 knockdown reduced transverse stiffness, with a prominent reduction in peak stiffness at high speeds of deformation ($E_{max}$) and viscoelasticity ($E\Delta$, rate-dependent stiffness) in cardiomyocytes from failing human hearts. Together, these data

are consistent with improved kinetics of failing ventricular cardiomyocytes conferred at least in part by reductions in viscoelasticity, due to depletion of VASH1 and reduction in detyrosinated microtubules.

## DISCUSSION

From the above data we come to the following conclusions: 1) the VASH1-SVBP complex acts as a primary tubulin carboxypeptidase in cardiomyocytes; 2) knockdown of VASH1 reduces cardiomyocyte stiffness and improves contractility, particularly in cardiomyocytes from patients with HF; and 3) targeting microtubule detyrosination specifically speeds cardiomyocyte relaxation, which does not require microtubule depolymerization or changes to the $Ca^{2+}$ transient. This work identifies new therapeutic targets for the modulation of cardiomyocyte relaxation and diastolic function.

This study represents the first examination of direct suppression of a tubulin carboxypeptidase in cardiomyocytes. Prior to the discovery of VASH-SVBP as a detyrosinating enzyme complex, the putative carboxypeptidase was commonly inhibited pharmacologically with parthenolide. While effective at high concentrations, parthenolide enacts multiple off target effects including alterations in calcium handling[5] and cellular signaling cascades.[10,21] Detyrosination can be genetically reduced by overexpression of the tyrosinating enzyme TTL, and like parthenolide, TTL overexpression reduces stiffness and improves contractility in human cardiomyocytes. Yet the mechanism of TTL action is confounded by the ability of TTL to depolymerize the microtubule network through its 1:1 interaction with free tubulin.[8,9] While mild depolymerization of the microtubule network might be acutely beneficial in improving cardiomyocyte contractility, chronic or gross depolymerization could lead to trafficking and signaling defects.[13,22] A TTL-based therapeutic approach is further complicated by a reliance on gene therapy to deliver TTL or the unlikely identification of a TTL agonist. In contrast, small molecule inhibitors of VASH1 or the VASH-SVBP interaction can be more readily designed based on recent structural studies of the complex[16–18] or identified using high-throughput screens, potentially facilitating translational studies. The role of VASH1 as a negative regulator of angiogenesis must be considered, but the vascular architecture of *Vash1* KO mice appears largely unchanged.[23]

VASH1 depletion had minor effects on the contractile profile of NF cardiomyocytes, with more robust effects on cardiomyocytes from patients with HF, particularly HFpEF where relaxation kinetics were dramatically slowed. Diastolic dysfunction is a hallmark of both HCM and HFpEF, where both intrinsic myocyte adaptations and extrinsic changes can impair myocardial relaxation.[1,2] Reducing cardiomyocyte stiffness and improving myocyte relaxation could reduce isovolumic relaxation times, increase ventricular compliance, and reduce diastolic pressures, all of which may benefit patients with diastolic dysfunction. Pharmacological approaches to promote myocyte relaxation and treat HCM are in development, including calcium desensitizers[24,25] and most notably with myosin inhibitors that have advanced to clinical trials.[26] Interestingly, myosin inhibitors speed relaxation proportional to a reduction in contractility, as do interventions that reduce myofilament calcium sensitivity. It is unclear if the therapeutic benefit of such approaches arises from the

faster relaxation, reduced systolic force production, or a net decrease in time under tension that may limit hypertrophic remodeling. Intriguingly, our results indicate an alternative, $Ca^{2+}$-independent mechanism to speed relaxation. Reducing viscoelasticity (energy loss) may speed cardiomyocyte relaxation without compromising systolic force production or increasing energetic demand, as would be the case for an increase in calcium cycling. How such a strategy would fit in the toolkit and compare to current approaches for treating different etiologies of diastolic or systolic dysfunction is of interest and will require extensive further study.

A limitation of the current work is the difficulty in quantifying protein levels of VASH/SVBP, which may be aided by further antibody refinement or targeted mass-spectrometry approaches. Additionally, protein expression does not speak to enzymatic activity directly, and little is known about post-translational regulation of these enzymes and the effect it has on detyrosinase activity.

These results provide the first demonstration of the effects of VASH1/SVBP inhibition on the intrinsic relaxation and viscoelasticity of isolated cardiomyocytes. This is a simplified system, and the diastolic pressure-volume relationship *in vivo* is influenced by numerous additional factors, including filling pressures that load and stretch cardiomyocytes. Of note, similar reductions in viscoelasticity with parthenolide or TTL overexpression equate to increased compliance of cardiomyocytes upon loaded cell stretch,[4] so we surmise the same will hold true for inhibition of VASH1. The current study prompts future investigations of the role of VASH1 in animal models of diastolic dysfunction, yet care must be taken in experimental design.

It is difficult to predict how chronic manipulations of TTL may affect cardiac function (or how effects will be interpreted), given the numerous potential consequences of altering microtubule detyrosination,[27] for example on autophagy,[28] oxidative stress,[13,29] and intracellular trafficking.[30–32] Further, it is unclear whether common murine models of heart failure recapitulate the cytoskeletal remodeling that occurs in patients with HCM and heart failure.[5–7] Studies utilizing small molecule inhibition or rapid, inducible depletion of VASH1 in models of diastolic dysfunction that recapitulate the patient cytoskeletal landscape will be most informative.

## Supplementary Material

Refer to Web version on PubMed Central for supplementary material.

## ACKNOWLEDGEMENT

The authors thank Dr. J. Chen for providing assistance and discussion on co-immunoprecipitation.

SOURCES OF FUNDING

This work was supported by funding from NHLBI grant R01-HL133080 to B.L.P., NIGMS 5T32HL007954-20 to A.K.S., NIAMS grant 5T32AR053461 to M.A.C., American Heart Association Fellowship 19POST34400012 to C.Y.C, Sanofi iAwards to B.L.P. and K.B.M., DZHK (German Centre of Cardiovascular Research) to L.C., the German Ministry of Research Education (BMBF) to L.C., the Deutsche Herzstiftung to S.S, and the Helmut und Charlotte Kassau Stiftung to L.C.

## Nonstandard Abbreviations and Acronyms:

| | |
|---|---|
| **HCM** | hypertrophic cardiomyopathy |
| **HF** | heart failure |
| **HFpEF** | heart failure with preserved ejection fraction |
| **HFrEF** | heart failure with reserved ejection fraction |
| **LV** | left ventricular |
| **NF** | non-failing |
| **SVBP** | small vasohibin binding protein |
| **TTL** | tubulin tyrosine ligase |
| **VASH1** | vasohibin 1 |

## REFERENCES


1. Rakowski H, Carasso S. Quantifying Diastolic Function in Hypertrophic Cardiomyopathy. Circulation. 2007;116:2662–2665. [PubMed: 18056537]
2. Borlaug BA, Paulus WJ. Heart failure with preserved ejection fraction: pathophysiology, diagnosis, and treatment. Eur Heart J. 2011;32:670–679. [PubMed: 21138935]
3. Robison P, Caporizzo MA, Ahmadzadeh H, Bogush AI, Chen C, Margulies KB, Shenoy VB, Prosser BL. Detyrosinated microtubules buckle and bear load in contracting cardiomyocytes. Science. 2016;352:aaf0659. [PubMed: 27102488]
4. Caporizzo M, Chen C, Salomon A, Margulies KB, Prosser BL. Microtubules provide a viscoelastic resistance to myocyte motion. Biophys J. 2018;115:1796–1807. [PubMed: 30322798]
5. Chen C, Caporizzo MA, Bedi K, Vite A, Bogush AI, Robison P, Heffler JG, Salomon AK, Kelly NA, Babu A, Morley MP, Margulies KB, Prosser BL. Suppression of detyrosinated microtubules improves cardiomyocyte function in human heart failure. Nat Med. 2018;24:1225–1233. [PubMed: 29892068]
6. Zile MR, Green GR, Schuyler GT, Aurigemma GP, Miller DC, Cooper G. Cardiocyte cytoskeleton in patients with left ventricular pressure overload hypertrophy. J Am Coll Cardiol. 2001;37:1080–1084. [PubMed: 11263612]
7. Dorsch LM, Schuldt M, dos Remedios CG, Schinkel A, de Jong PL, Michels M, Kuster D, Brundel B, van der Velden J. Protein Quality Control Activation and Microtubule Remodeling in Hypertrophic Cardiomyopathy. Cells. 2019;8:741.
8. Szyk A, aconescu A, Piszczek G, Roll-Mecak A. Tubulin tyrosine ligase structure reveals adaptation of an ancient fold to bind and modify tubulin. Nat Struct Mol Biol. 2011;18:1250. [PubMed: 22020298]
9. Nieuwenhuis J, Brummelkamp TR. The Tubulin Detyrosination Cycle: Function and Enzymes. Trends Cell Biol. 2018;29:80–92. [PubMed: 30213517]
10. Wen J, You K-R, Lee S-Y, Song C-H, Kim D-G. Oxidative Stress-mediated Apoptosis THE ANTICANCER EFFECT OF THE SESQUITERPENE LACTONE PARTHENOLIDE. J Biol Chem. 2002;277:38954–38964. [PubMed: 12151389]
11. Aillaud C, Bosc C, Peris L, Bosson A, Heemeryck P, Dijk J, Friec J, Boulan B, Vossier F, Sanman LE, Syed S, Amara N, Couté Y, Lafanechère L, Denarier E, Delphin C, Pelletier L, Humbert S, Bogyo M, Andrieux A, Rogowski K, Moutin M-J. Vasohibins/SVBP are tubulin carboxypeptidases (TCPs) that regulate neuron differentiation. Science. 2017;358:1448–1453. [PubMed: 29146868]

12. Nieuwenhuis J, Adamopoulos A, Bleijerveld OB, Mazouzi A, Stickel E, Celie P, Altelaar M, Knipscheer P, Perrakis A, Blomen VA, Brummelkamp TR. Vasohibins encode tubulin detyrosinating activity. Science. 2017;358:1453–1456. [PubMed: 29146869]
13. Prosser BL, Ward CW, Lederer W. X-ROS Signaling: Rapid Mechano-Chemo Transduction in Heart. Science. 2011;333:1440–1445. [PubMed: 21903813]
14. Heffler J, Shah PP, Robison P, Phyo S, Veliz K, Uchida K, Bogush A, Rhoades J, Jain R, Prosser BL. A Balance Between Intermediate Filaments and Microtubules Maintains Nuclear Architecture in the Cardiomyocyte. Circ Res. 2019;
15. Singh SR, Zech A, Geertz B, Reischmann-Düsener S, Osinska H, Prondzynski M, Krämer E, Meng Q, Redwood C, van der Velden J, Robbins J, Schlossarek S, Carrier L. Activation of Autophagy Ameliorates Cardiomyopathy in Mybpc3-Targeted Knockin Mice. Circulation Hear Fail. 2018;10:e004140.
16. Wang N, Bosc C, Choi S, Boulan B, Peris L, Olieric N, Bao H, Krichen F, Chen L, Andrieux A, Olieric V, Moutin M-J, Steinmetz MO, Huang H. Structural basis of tubulin detyrosination by the vasohibin–SVBP enzyme complex. Nat Struct Mol Biol. 2019;1–12. [PubMed: 30559461]
17. Li F, Hu Y, Qi S, Luo X, Yu H. Structural basis of tubulin detyrosination by vasohibins. Nat Struct Mol Biol. 2019;26:583–591. [PubMed: 31235910]
18. Liao S, Rajendraprasad G, Wang N, Eibes S, Gao J, Yu H, Wu G, Tu X, Huang H, Barisic M, Xu C. Molecular basis of vasohibins-mediated detyrosination and its impact on spindle function and mitosis. Cell Res. 2019;1–15. [PubMed: 30514898]
19. van der Laan S, Lévêque MF, Marcellin G, Vezenkov L, Lannay Y, Dubra G, Bompard G, Ovejero S, Urbach S, Burgess A, Amblard M, Sterkers Y, Bastien P, Rogowski K. Evolutionary Divergence of Enzymatic Mechanisms for Tubulin Detyrosination. Cell Reports. 2019;29:4159–4171.e6. [PubMed: 31851940]
20. Andrieux A, Moutin M-J, Bosc C, Aillaud C, Peris L, Delagrange P, inventors; INSERM, Universite Grenoble Alpes, Commissariat A L'energie Atomique Et Aux Energies Alternatives, Les Laboratoires Servier, assignees. Methods and pharmaceutical compositions for treating tubulin carboxypeptidases associated diseases. World International Patent Number: PCT/EP2018/079448 2018 10 26.
21. Ghantous A, Sinjab A, Herceg Z, Darwiche N. Parthenolide: from plant shoots to cancer roots. Drug Discov Today. 2013;18:894–905. [PubMed: 23688583]
22. Shaw RM, Fay AJ, Puthenveedu MA, von Zastrow M, Jan Y-N, Jan LY. Microtubule Plus-End-Tracking Proteins Target Gap Junctions Directly from the Cell Interior to Adherens Junctions. Cell. 2007;128:547–560. [PubMed: 17289573]
23. Kimura H, Miyashita H, Suzuki Y, Kobayashi M, Watanabe K, Sonoda H, Ohta H, Fujiwara T, Shimosegawa T, Sato Y. Distinctive localization and opposed roles of vasohibin-1 and vasohibin-2 in the regulation of angiogenesis. Blood. 2009;113:4810–4818. [PubMed: 19204325]
24. Tadano N, Du C, Yumoto F, Morimoto S, Ohta M, Xie M, Nagata K, Zhan D, Lu Q, Miwa Y, Takahashi-Yanaga F, Tanokura M, Ohtsuki I, Sasaguri T. Biological actions of green tea catechins on cardiac troponin C. Brit J Pharmacol. 2010;161:1034–1043. [PubMed: 20977454]
25. Adhikari BB, Wang K. Interplay of Troponin- and Myosin-Based Pathways of Calcium Activation in Skeletal and Cardiac Muscle: The Use of W7 as an Inhibitor of Thin Filament Activation. Biophys J. 2004;86:359–370. [PubMed: 14695278]
26. Green EM, Wakimoto H, Anderson RL, Evanchik MJ, Gorham JM, Harrison BC, Henze M, Kawas R, Oslob JD, Rodriguez HM, Song Y, Wan W, Leinwand LA, Spudich JA, well RS, Seidman J, Seidman CE. A small-molecule inhibitor of sarcomere contractility suppresses hypertrophic cardiomyopathy in mice. Science. 2016;351:617–621. [PubMed: 26912705]
27. Caporizzo MA, Chen C, Prosser BL. Cardiac microtubules in health and heart disease. Exp Biol Med. 2019;153537021986896.
28. Mohan N, Sorokina EM, Verdeny I, Alvarez A, Lakadamyali M. Detyrosinated microtubules spatially constrain lysosomes facilitating lysosome–autophagosome fusion. J Cell Biol. 2018;218:jcb.201807124.

29. Kerr JP, Robison P, Shi G, Bogush AI, Kempema AM, Hexum JK, Becerra N, Harki DA, Martin SS, Raiteri R, Prosser BL, Ward CW. Detyrosinated microtubules modulate mechanotransduction in heart and skeletal muscle. Nat Commun. 2015;6:8526. [PubMed: 26446751]

30. Sirajuddin M, Rice LM, Vale RD. Regulation of microtubule motors by tubulin isotypes and post-translational modifications. Nat Cell Biol. 2014;16:335–344. [PubMed: 24633327]

31. Barisic M, e Sousa R, Tripathy SK, Magiera MM, Zaytsev AV, Pereira AL, Janke C, Grishchuk EL, Maiato H. Microtubule detyrosination guides chromosomes during mitosis. Science. 2015;348:799–803. [PubMed: 25908662]

32. Hammond JW, Huang C-F, Kaech S, Jacobson C, Banker G, Verhey KJ. Posttranslational Modifications of Tubulin and the Polarized Transport of Kinesin-1 in Neurons. Mol Biol Cell. 2010;21:572–583. [PubMed: 20032309]

## NOVELTY AND SIGNIFICANCE

**What Is Known?**

- Microtubules, a major component of the cytoskeleton, contribute to the passive mechanics of cardiomyocytes and can resist cardiomyocyte shortening and re-lengthening.
- Posttranslational detyrosination of tubulin increases this resistance to motion and is elevated in human heart failure, which increases stiffness and impairs contractility in failing cardiomyocytes.
- A detyrosinating enzyme complex of vasohibins and small vasohibin binding protein (VASH/SVBP) was recently identified in non-muscle cell types, yet the active detyrosinase in cardiomyocytes remained unknown.

**What New Information Does This Article Contribute?**

- We identify VASH1/SVBP as a primary detyrosinase in cardiomyocytes.
- Depletion of VASH1 reduces stiffness and improves contractile function in cardiomyocytes from patient with heart failure with preserved or reduced ejection fraction (HFpEF or HFrEF, respectively).
- Targeting tubulin detyrosination specifically speeds cardiomyocyte relaxation, independent of changes to calcium cycling, supporting pursuit of VASH1/SVBP as a novel therapeutic target in heart failure.

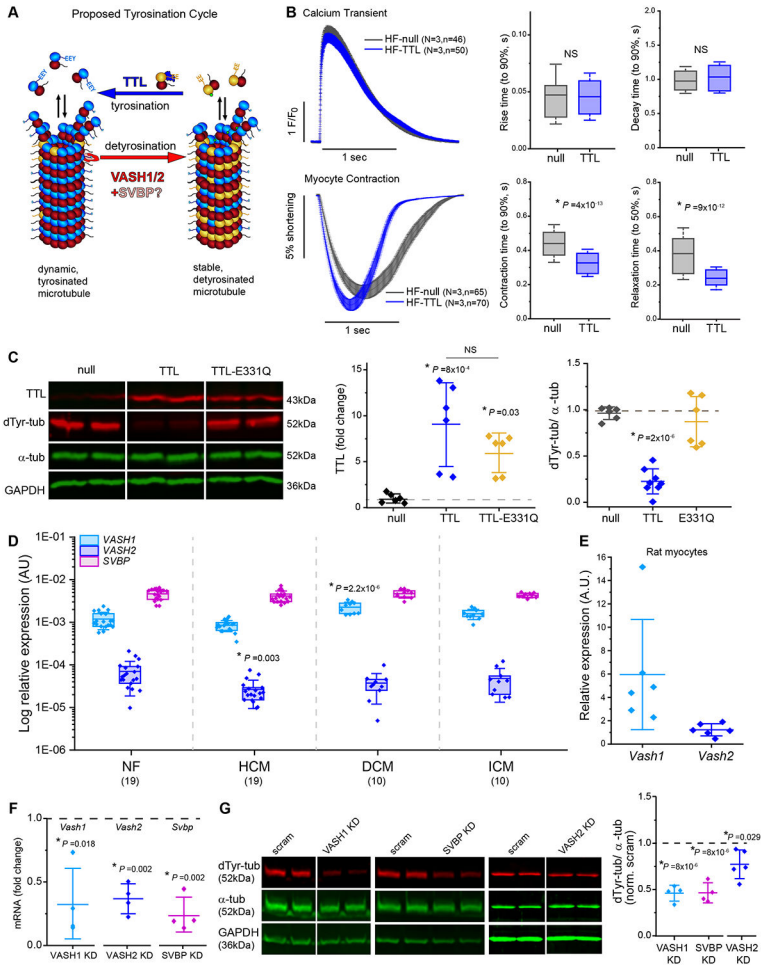


**Figure 1. Identification of the primary cardiac detyrosinase and development of tools to probe the tyrosination cycle.**

**A**, Schematic of proposed microtubule tyrosination cycle in cardiomyocytes. **B**, Average traces of electrically stimulated $[Ca^{2+}]_i$ transients (top) and sarcomere shortening (bottom) from failing human cardiomyocytes infected with a null (grey) or TTL-encoding (blue) adenovirus. Traces depict change in signal normalized to resting fluorescence ($F_0$) or resting length. Kinetic parameters of calcium transients and sarcomere shortening are quantified to the right. Statistical significance determined via two-sided t-tests with Bonferroni correction for two comparisons, unadjusted P value are shown * vs. null. **C**, Validation of TTL-E331Q construct. Representative western blot and quantification of TTL, detyrosinated tubulin (dTyr-tub), α-tubulin (α-tub), and GAPDH levels in whole cell extracts from isolated rat cardiomyocytes expressing null, TTL, or TTL-E331Q constructs. Statistical significance determined via one-way analysis of variance (ANOVA) with post-hoc Bonferroni test from duplicates of N=3 rat hearts, * vs. null. **D**, Expression profiling of *VASH1*, *VASH2* and *SVBP* genes via RT-qPCR of patient myocardial samples. Statistical significance determined via one-way ANOVA with post-hoc Bonferroni test, * vs. NF. **E**, Expression levels of *Vash1* and *Vash2* in isolated rat cardiomyocytes. **F**, Validation of knockdown (KD) via RT-qPCR quantification of *Vash1*, *Vash2*, and *Svbp* in rat cardiomyocytes. **G**, Representative western blot and quantification of detyrosinated tubulin, α-tubulin, and GAPDH levels from isolated

rat cardiomyocytes treated with different concentrations of adenovirus encoding SVBP or VASH1 KD constructs. Data presented as fold change from scramble (scram) control. Statistical significance determined via two-sided Student's t-tests for RT-qPCR (**F**) and VASH2 KD western blot (**G**), and via one-way ANOVA for VASH1 and SVBP KD western blot, * vs. scram. Data are presented as mean ± s.d. if not otherwise specified.

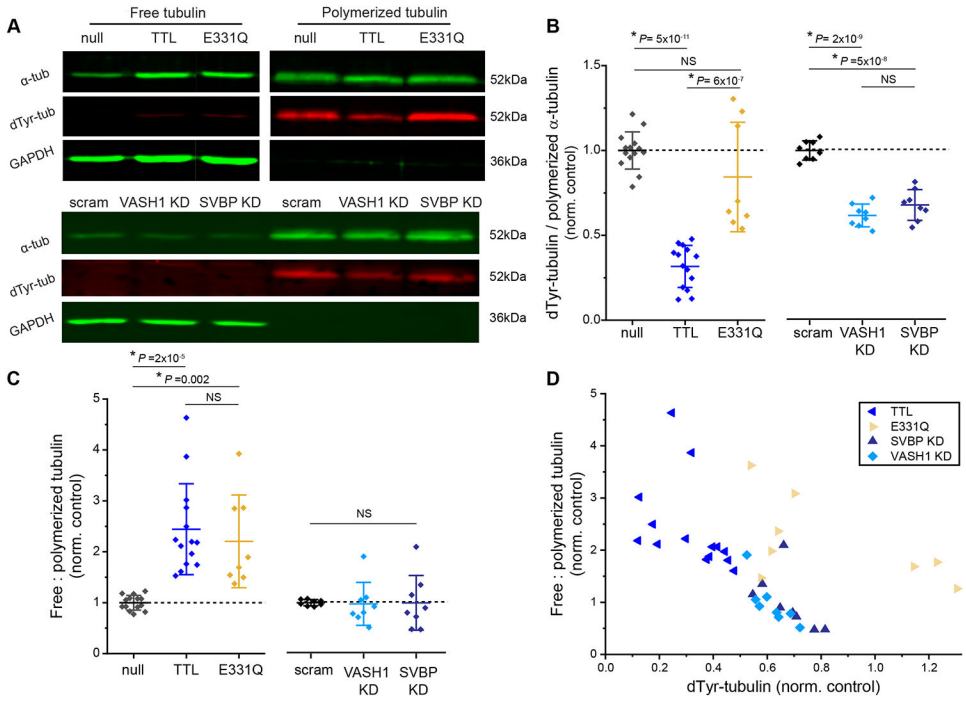


**Figure 2. TTL tubulin sequestration, but not detyrosination, depolymerizes microtubules in healthy cardiomyocytes.**

**A**, Representative western blot of free and polymerized tubulin from isolated rat cardiomyocytes transduced with adenoviruses encoding null, TTL, TTL-E331Q, scram, VASH1 KD and SVBP KD. Quantification of (**B**) detyrosinated tubulin level found in the polymerized fraction and (**C**) free to polymerized tubulin ratio. Statistical significance determined via one-way ANOVA with post-hoc Bonferroni test, * vs. null or scram, with duplicates of N=7 rat hearts for null and TTL and duplicates of N=4 for TTL-E331Q, scram, VASH1 KD, and SVBP KD. **D**, Correlation between detyrosinated tubulin levels found in the polymerized fraction and the ratio of free:polymerized tubulin.

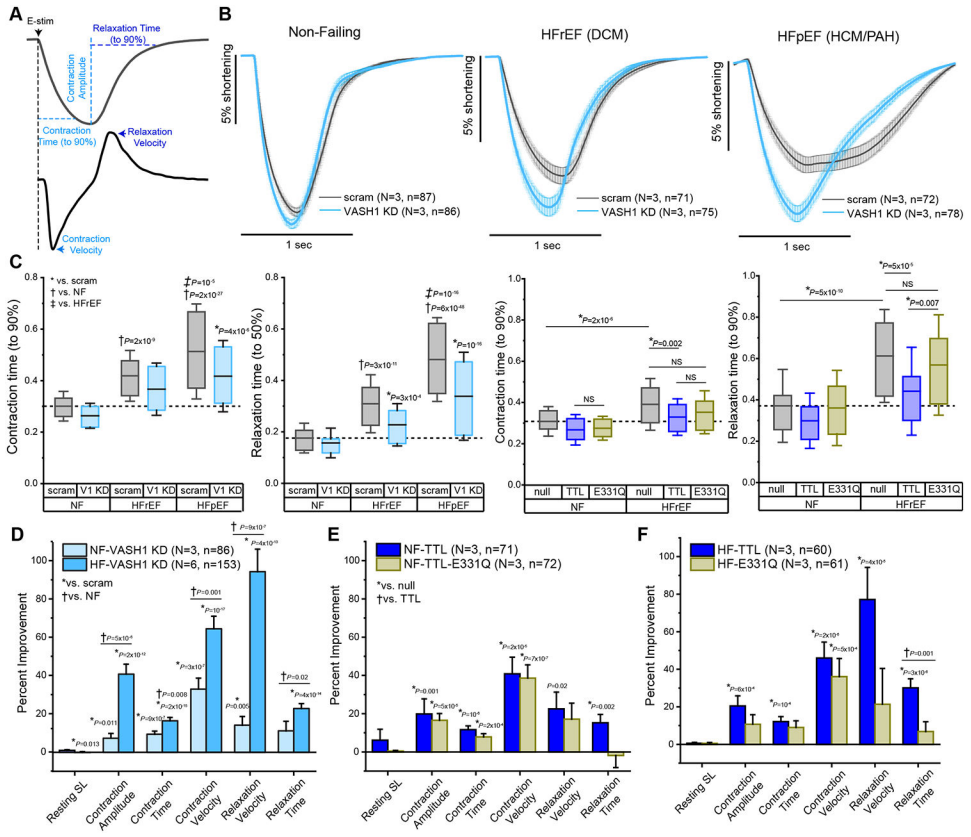


**Figure 3. Reducing detyrosination speeds contraction and relaxation of failing human cardiomyocytes.**

**A**, Example of sarcomere shortening trace from myocyte responding to electrical stimulation and corresponding first derivative identifying key contractile parameters collected. **B**, Average traces of sarcomere shortening from cardiomyocytes isolated from NF donor hearts and from hearts from patients with HFrEF and HFpEF, with or without VASH1 KD. **C**, Contraction and relaxation times are quantified and grouped by etiology and experimental conditions. Statistical significance determined via two-way ANOVA between the effects of etiology and treatment. *P* values for significant interactions are shown. For detailed two-way ANOVA report, see Online Table III. **D** through **F**, Percent improvement in contractile parameters by each genetic manipulation over null or scram is quantified and grouped by etiology and experimental conditions. **D**, statistical significance determined via two-sided Student's t-tests with Bonferroni correction for six comparisons (adjusted $\alpha$=0.05/6=0.0083), unadjusted P values are shown * vs. scram and † vs. NF. **E** and **F**, Statistical significance determined via two-sided Student's t-tests with Bonferroni correction for six comparisons (adjusted=0.0083), unadjusted P values are shown * vs. null and † vs. TTL of that etiology. Data are presented as mean ± s.e.m. in bar graphs (**D** and **F**).

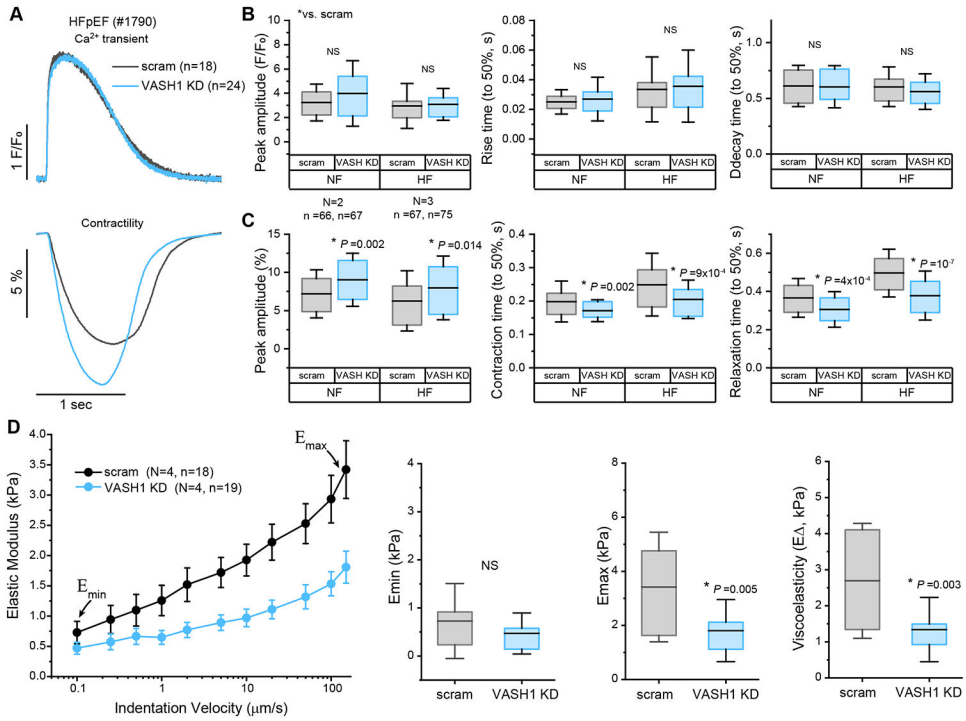


**Figure 4. VASH1 knockdown reduces myocyte viscoelasticity and improves contractility independent of changes to the calcium transient.**

**A**, Average traces of simultaneously acquired $[Ca^{2+}]_i$ transients and sarcomere shortening from fluo-3 loaded cardiomyocytes isolated from the heart of patient #1790 with heart failure with preserved ejection fraction (HFpEF). Traces are normalized to baseline fluorescence ($F_0$) and sarcomere length, respectively. Amplitude and kinetic parameters from $[Ca^{2+}]_i$ transients (**B**) and sarcomere shortening (**C**) were quantified simultaneously in cardiomyocytes isolated from NF or failing hearts with or without VASH1 KD. Statistical significance determined via two-sided t-tests with Bonferroni correction for three comparisons (adjusted $\alpha$=0.05/3=0.017), unadjusted P values are shown * vs. scram of that etiology. **D**, Nanoindentation measurements of viscoelasticity. Stiffness (elastic modulus) of failing cardiomyocytes as a function of probe indentation velocity with or without VASH1 KD. Quantification of $E_{min}$, $E_{max}$ and viscoelasticity ($E\Delta$) in right panels. Statistical significance determined via two-sided t-tests for three comparisons (adjusted $\alpha$=0.017), unadjusted P values are shown *vs. scram. Data are presented as mean ± s.e.m. in (**D**) left panel.

**Table 1.**

Summary descriptive statistics of human hearts used in this study.

| Etiology | No. of hearts | Age (year) | LVMI (g/m$^2$) | LVEF (%) |
|---|---|---|---|---|
| NF | 2M, 4F | 54.83 ± 6.09 | 101.03 ± 8.96 | 58.33 ± 5.27 |
| HFpEF | 3M, 3F | 52.17 ± 5.06 | 150.26 ± 10.96 | 67.5 ± 2.81 |
| HFrEF | 6M, 4F | 48.1 ± 3.75 | 116.18 ± 6.49 | 18 ± 1.53 |

Each value is presented as mean ± s.e.m. Abbreviations: F, female; LVMI, left ventricular mass index; M, male.